

Experimental constraints on the sources of lithium-rich granites and pegmatites

Bence Horányi^{1*}, Austin M. Gion^{1,2}, Fabrice Gaillard¹, Éric Gloaguen^{1,3}, Alexis Plunder³, Jérémie Melleton³, Alban Moradell-Casellas^{1,3}, Josselyn Garde¹, Saskia Erdmann¹, Ida Di Carlo¹

¹Institute des Sciences de la Terre d'Orléans, UMR 7327, Univ. Orléans, CNRS, BRGM, OSUC, F-45071, Orléans, France

²Department of Earth Sciences, University of Oxford, OX1 3AN, Oxford, UK

³Bureau de Recherches Géologiques et Minières, F-45060, Orléans, France

**e-mail: bence.horanyi@cnrs-orleans.fr*

Supplementary Note

Geochemical database (Fig. 1b). The geochemical composition of sedimentary rocks was compiled from the Sedimentary Geochemistry and Paleoenvironments (SGP) Project dataset¹ (Supplementary Data 2). The SGP database was filtered for siliciclastic, volcano-sedimentary, and evaporitic deposits (n = 10015). The volcano-sedimentary deposit in Jadar, Serbia (8360 ppm lithium²) and lithium-rich bauxites (up to 8200 ppm lithium³) were added to the database to highlight the most enriched sedimentary rocks that are observed in nature (n = 628). The geochemical composition of metamorphic and granitic rocks was derived from the GEOROC database (<https://georoc.eu/>) on the 3rd of June, 2024. The metamorphic rocks were filtered for metasedimentary rocks and gneisses (n = 1481), which are considered to be fertile sources of peraluminous, granitic melts^{4,5}. Enriched metabauxites (up to 2290 ppm lithium) from Goffé⁶,

Franceschelli et al.⁷, and Verlaquet et al.⁸ were also added to the database (n = 37). Lithium may become enriched in metamorphic rocks during supergene processes⁹; therefore, altered metasedimentary rocks were removed from the database. The granitic dataset was filtered for peraluminous granites (n = 3059), which may form by the partial melting of crustal rocks^{4,5}. The composition of rare-metal granites was obtained from Linnen and Cuney¹⁰ and references therein (n = 86). Only the peraluminous, high-phosphorous (PHP) rare-metal granites were considered, which are interpreted to have a metasedimentary source¹⁰. Rare-metal pegmatites, including Tanco¹¹, Greenbushes¹², Chèdeville¹³, Wabouchi¹⁴, and Kamativi¹⁵ were subsequently added to this dataset (n = 68). Rare-metal granites and pegmatites often undergo late-stage hydrothermal alteration, which may alter the lithium budget of the system^{16,17}. The effect of hydrothermal alteration on the lithium budget of RMGPs is poorly constrained; therefore, altered deposits were also included in the RMGP dataset. In contrast, the extrusive equivalent of RMGPs, termed rare-metal rhyolites, are considered to be unaltered by late-stage hydrothermal processes¹⁸⁻²⁰. There are only two known examples of peraluminous, high-phosphorous rare-metal rhyolites in nature, namely the Macusani volcanics^{18,19} and the Richemont rhyolite²⁰. Rare-metal rhyolites, granites, and pegmatites are inherently over-represented in the geochemical database due to their economic significance. Furthermore, metasedimentary rocks are under-represented relative to peraluminous granites due to a sampling bias towards the latter.

Supplementary Discussion

The stability of staurolite during crustal anatexis. Staurolite is typically considered to be absent during crustal anatexis due to its subsolidus breakdown at ~650°C during Barrovian metamorphism, according to schematic equation S1²¹:



Nevertheless, there are several lines of evidence to suggest that staurolite can contribute to melting reactions during the anatexis of metapelites. Firstly, the incorporation of Al, Zn, and Li into staurolite can considerably enhance its stability field in lithium-rich metasedimentary rocks²²⁻²⁴. Secondly, staurolite melting reactions have been texturally documented in the Barr888 and the FM1 experimental run products (Fig. 3e and Supplementary Fig. 2. Thirdly, several experimental²⁴⁻²⁸ and numerical²⁹⁻³¹ studies have demonstrated that staurolite can contribute to melt formation or remain stable above the solidus (up to 855°C) during the fluid-present or fluid-absent partial melting of metapelites. The contribution of staurolite to melting reactions is enhanced during fluid-present melting, due to the pronounced effect of excess fluids on the solidus of metapelitic systems (<700°C)²⁴. Fourthly, staurolite may remain metastable following subsolidus breakdown due to its sluggish dissolution²¹, akin to the partial melting experiments in this study. Therefore, metastable staurolite may contribute to melting reactions if the temperature difference between staurolite breakdown and the solidus is low³¹. In summary, experimental, analytical, and numerical studies demonstrate that staurolite can contribute to melting reactions during crustal anatexis, particularly in lithium-rich metasedimentary rocks. This reaction is likely under-represented in the geological record due to the narrow stability field of staurolite and its progressive consumption during partial melting^{24,28}.

Approach to equilibrium. Partial melting and crystallisation experiments at <800°C have demonstrated that kinetics are sluggish in low-temperature felsic systems^{21,27,32-34}. Therefore, the attainment of equilibrium between minerals and melts in experimental and natural anatectic settings has been questioned by several studies³⁵⁻⁴¹. For example, the partial melting experiments of Acosta-Vigil et al.⁴⁰ demonstrate that the dissolution of minerals is limited to

their interface and produces disequilibrium melts. Although such studies provide important constraints on melting reactions during anatexis, there are several geochemical and textural observations which demonstrate an approach to equilibrium between residual minerals and melts in the partial melting experiments. Firstly, mineral-melt partition coefficients of rare metals (e.g., Li, Rb, Nb, Ta, and W) are comparable between residual and newly crystallised biotite from GAR 01 and GAR 15, respectively (Table 3 and Table S9 in Supplementary Data 1). The partition coefficient of caesium between biotite and melt is slightly higher in the melting experiments than in the crystallisation experiments; therefore, the caesium content of the GAR 01 glasses is interpreted to be a lower estimate of enrichment. Secondly, textural (Figs. 1 and 3) and compositional (Table 3; Tables S6 and S7 in Supplementary Data 1) differences are observed between residual minerals in the run products and the starting materials, which is consistent with previous experimental studies^{5,24,27,34,42-44} and natural anatectic enclaves^{45,46}. The depletion of rare metals in residual minerals relative to their starting composition demonstrates that melting reactions are not limited to crystal rims; therefore, bulk partition coefficients of rare metals are <1 (Table 2). Thirdly, rare metals behave as trace elements and obey Henry's law in all major and accessory phases that are observed in the experiments, as well as in lithium-undersaturated rhyolites, migmatites, and metapelites in nature³⁷. Fourthly, the major element composition of glasses is consistent between experiments of varying timescales (48 to 430 hours; Supplementary Fig. 4). Lastly, the trace element compositions of minerals and glasses are homogenous in the run products (Tables S8-S11 in Supplementary Data 1), which demonstrates the equilibration of rare metals by diffusion³⁴.

The applicability of experimental studies to natural systems and the attainment of chemical equilibrium in migmatites is further supported by the fast diffusivity of Li, Rb, and Cs. Brown et al.³⁶ proposed that trace elements can achieve equilibrium distribution between

residual minerals and melts if their diffusivity is faster than $10^{-17} \text{ m}^2\text{s}^{-1}$ at 800°C . Alkali metals diffuse at least an order of magnitude faster than this threshold ($\sim 10^{-10} \text{ m}^2\text{s}^{-1}$ to $\sim 10^{-16} \text{ m}^2\text{s}^{-1}$ at 800°C)⁴⁷; therefore, chemical equilibrium is inferred between residual minerals and partial melts. Lithium is a light element that diffuses particularly fast in felsic systems. At 800°C , the diffusion distance of lithium in partial melts is $>26 \text{ cm/year}$ ^{34,48}, which is considerably faster than the rate of residual melt extraction in migmatites ($\sim 1\text{-}2 \text{ cm/year}$)³⁵. The equilibration of lithium between minerals and melts is further supported by the fast diffusivity of lithium in residual phases. For example, Charlier et al.⁴⁹ demonstrated that lithium equilibrates in plagioclase on a scale of minutes to hours at 737°C in crystals that are up to $\sim 500 \text{ }\mu\text{m}$ in size. In contrast to the alkali metals, Nb, Ta, and W diffuse notably slower in residual minerals and melts. However, these high-field strength elements are primarily hosted in newly crystallising minerals (magnetite and rutile), wherein equilibrium partitioning is inferred³⁷. Consequently, the effect of disequilibrium partitioning between residual minerals and melts on the Nb, Ta, W content of the extracted partial melts is negligible. These observations highlight that equilibrium mineral-melt partition coefficients of rare metals accurately capture trace element behaviour during crustal anatexis.

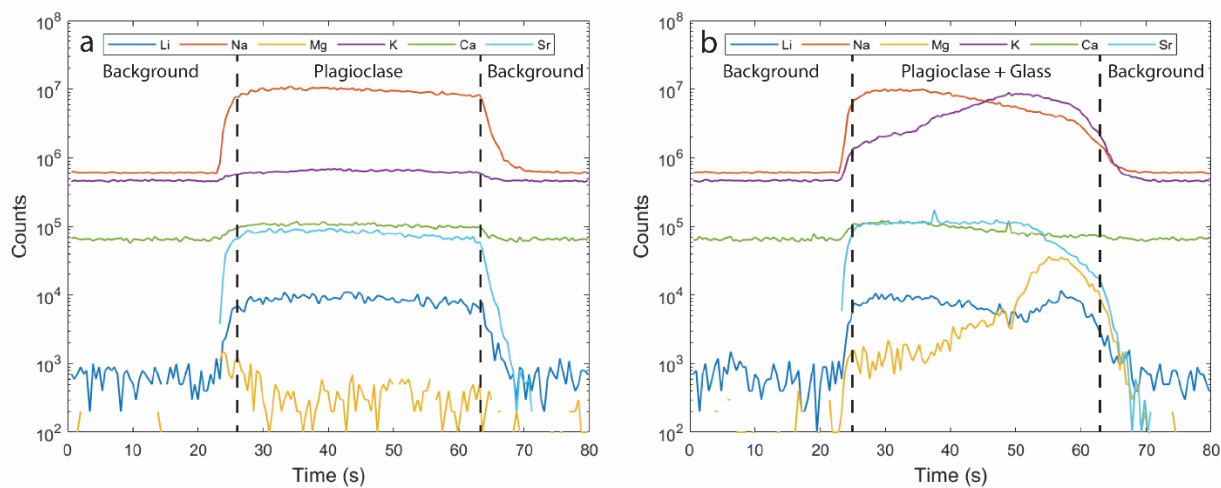
The anatexis of conventional metasedimentary rocks. To demonstrate the petrogenesis of common peraluminous granites in the crust ($<100 \text{ ppm}$ lithium), the anatexis of conventional metasedimentary rocks (20 ppm lithium; Fig. 1b) was simulated using a modal batch melting model (equation (6)) and the range of bulk partition coefficients from Fig. 7c ($\bar{D}_{Li} = 0.09$ to 0.21). The low-degree partial melting ($<10\%$) of conventional metasedimentary rocks produces partial melts with up to $\sim 120 \text{ ppm}$ lithium (Supplementary Fig. 7, which is comparable to anatectic enclaves and migmatites in nature^{45,50}). Assuming that the partitioning behaviour of lithium is similar during anatexis and fractionation, the high-degree fractional

crystallisation (>90%) of conventional peraluminous granites in the crust (~25 ppm lithium; Fig. 1b) would also produce felsic melts that contain <150 ppm lithium. The enrichment of lithium in the residual melts is comparable to highly fractionated rhyolites observed in nature⁵¹. To test whether lithium-poor parental melts can source RMGPs, the magmatic differentiation of the extracted anatectic melts (120 ppm lithium) was modelled (equation (6); Supplementary Fig. 7). The re-melting of granitic cumulates or the high-degree fractional crystallisation (>90%) of extracted melts may produce granitic rocks with up to 720 ppm lithium (Supplementary Fig. 7), which are depleted by up to an order of magnitude relative to economic grade RMGPs (>5000 ppm lithium). The extraction of these highly fractionated melts, followed by a third stage of magmatic differentiation (>90% fractionation or <10% melting) would again produce residual melts that are depleted relative to economic grade RMGPs (up to 4320 ppm lithium; Supplementary Fig. 7). The modelled results demonstrate that the low-degree partial melting (<10%) of conventional metasedimentary rocks (~20 ppm), and the two-stage high-degree fractional crystallisation (>90%) of the extracted melts is unlikely to produce RMGPs. Therefore, the crustal sources of RMGPs must be pre-enriched, which is consistent with the experimental results in this study.

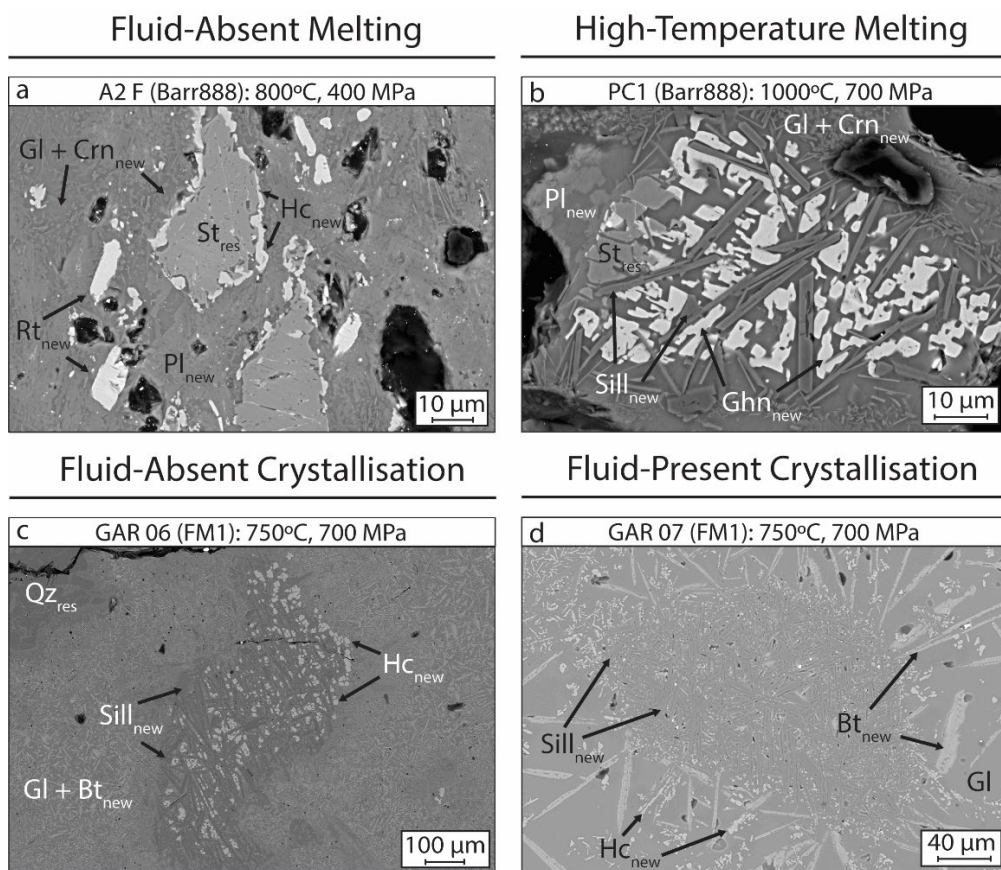
The enrichment of rare metals during crustal anatexis. The enrichment of rubidium and caesium during the anatexis of the FM1 micaschist was calculated using a modal batch melting model (equation (6)), assuming the complete breakdown of staurolite and biotite (Supplementary Fig. 8). The resulting bulk partition coefficients of rubidium and caesium range between 0.01-0.16 and 0.01-0.08, respectively (Table S13 in Supplementary Data 1). Following the complete breakdown of biotite, rubidium and caesium may become enriched by up to a factor of ~10 during low-degree (~10%) anatexis. The produced partial melts contain up to ~2500 ppm rubidium and ~600 ppm caesium, which is comparable to rare-metal

rhyolites¹⁸⁻²⁰ and the most evolved unit of the Beauvoir Granite (B1)⁵². In contrast, the anatexis of weakly enriched crustal rocks, such as the Barr888 metabauxite (80 ppm rubidium and 8.1 ppm caesium) produces a melt with up to 800 ppm rubidium and 80 ppm caesium (assuming an enrichment factor of 10), which is depleted relative to high-grade RMGP deposits. The modelled results demonstrate the significance of rare metal enrichment in the crustal source and the importance of biotite breakdown to maximise rubidium and caesium enrichment during crustal anatexis. Partial melts produced by the anatexis of weakly enriched crustal rocks (e.g., the Barr888 metabauxite), must become further enriched by fractional crystallization¹⁹ or late-stage metasomatic processes⁵³ to produce RMGPs.

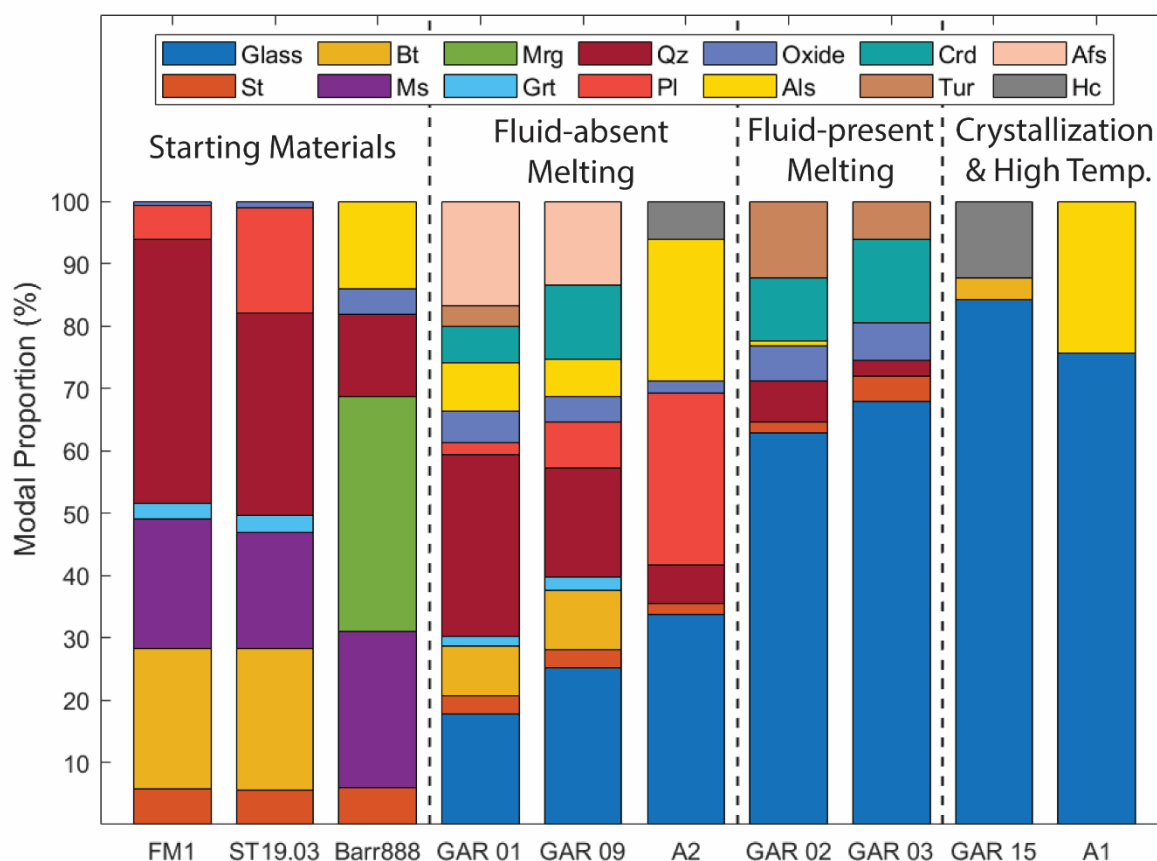
The enrichment or depletion of Nb, Ta, and W during anatexis was not considered in the trace element model due to the sensitivity of the calculations as a function of the modal proportion of oxides. Furthermore, partition coefficients of niobium and tantalum in rutile vary markedly as a function of rutile composition⁵⁴, which results in high degrees of uncertainty in the model. Tin is also enriched in RMGPs; however, it was not considered in this study due to the loss of tin to capsule walls during the experiments⁵⁵.



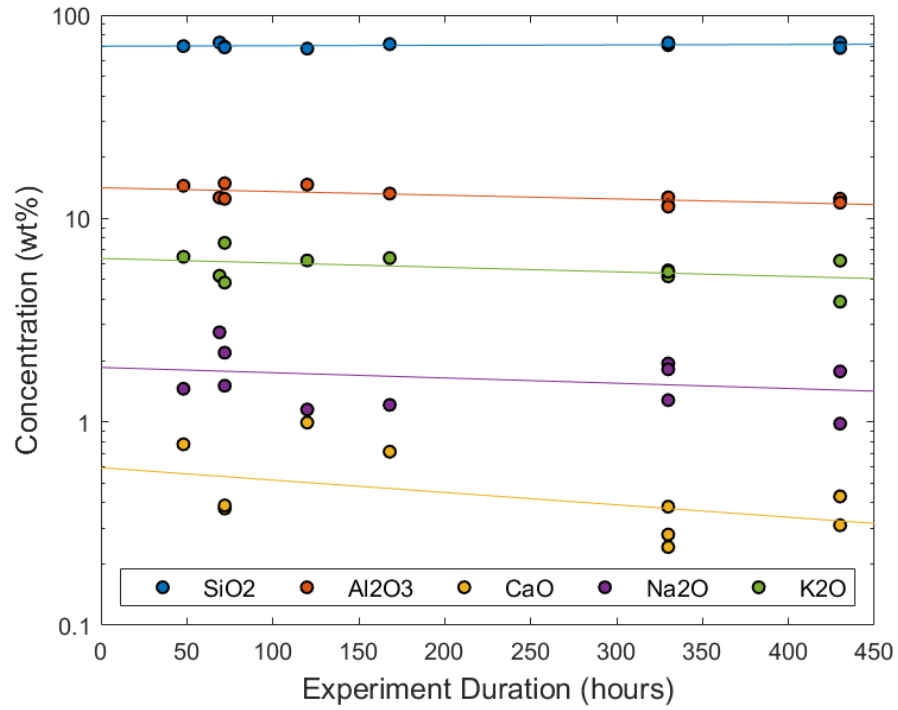
Supplementary Fig. 1 Representative analyses of trace elements in plagioclase by LA-ICP-MS. a. Analysis of residual plagioclase. **b.** Contamination of residual plagioclase analyses by glass, which results in fluctuations of trace elements.



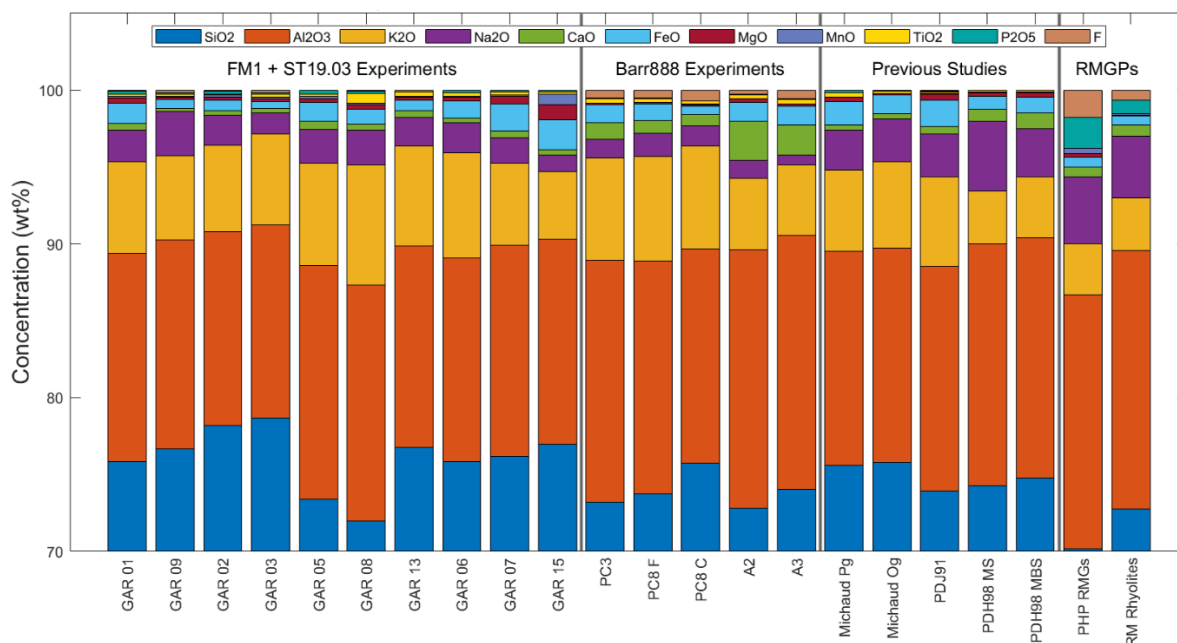
Supplementary Fig. 2 Representative SEM images of staurolite melting reactions observed in the experiments. Replacement or complete breakdown of metastable staurolite to sillimanite, hercynite/gahnite, and melt pseudomorphs in the **a.** fluid-absent melting experiments, **b.** high-temperature melting experiments, **c.** fluid-absent crystallisation experiments, and **d.** fluid-present crystallisation experiments. Mineral abbreviations are: Bt = biotite, Crn = corundum, Ghn = gahnite, Gl = glass, Hc = hercynite, Pl = plagioclase, Qz = quartz, Rt = rutile, Sill = sillimanite. ‘res’ denotes residual phases, whereas ‘new’ signifies newly crystallised minerals.



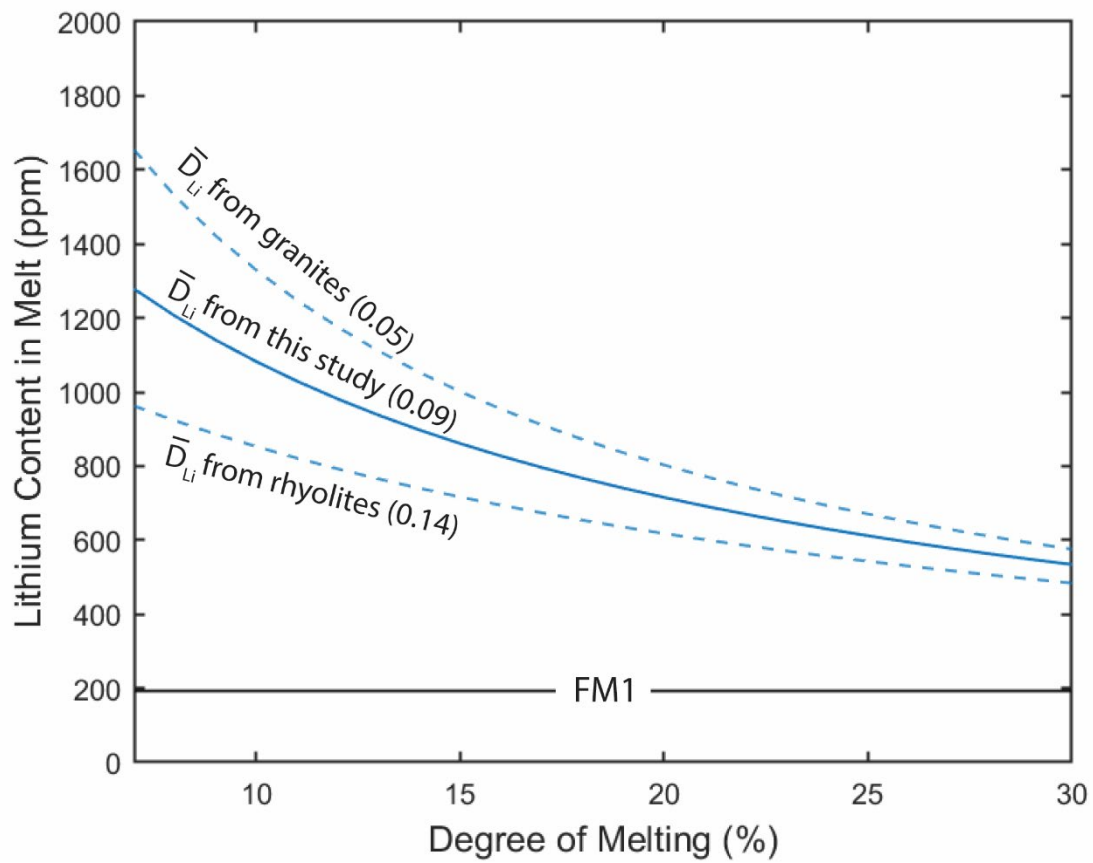
Supplementary Fig. 3 The modal mineralogy of the starting materials and the experimental run products. Mineral abbreviations are: St = staurolite, Bt = biotite, Ms = muscovite, Mrg = margarite, Grt = garnet, Qz = quartz, Pl = plagioclase, Als = aluminosilicates (including sillimanite, pyrophyllite, and corundum), Crd = cordierite, Tur = tourmaline, Afs = alkali feldspar, Hc = hercynite. The oxides include ilmenite, rutile, and magnetite.



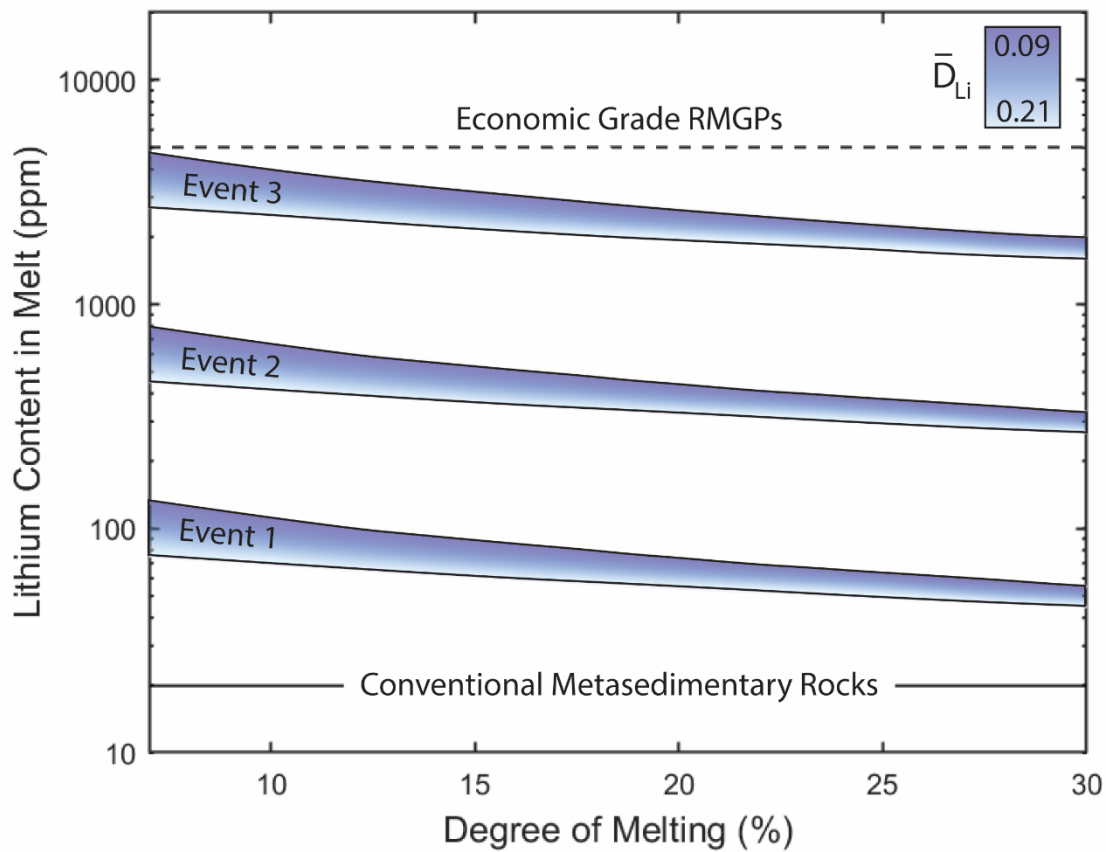
Supplementary Fig. 4 The major element composition of glasses as a function of experiment duration. The lack of compositional variability over time demonstrates an approach to equilibrium.



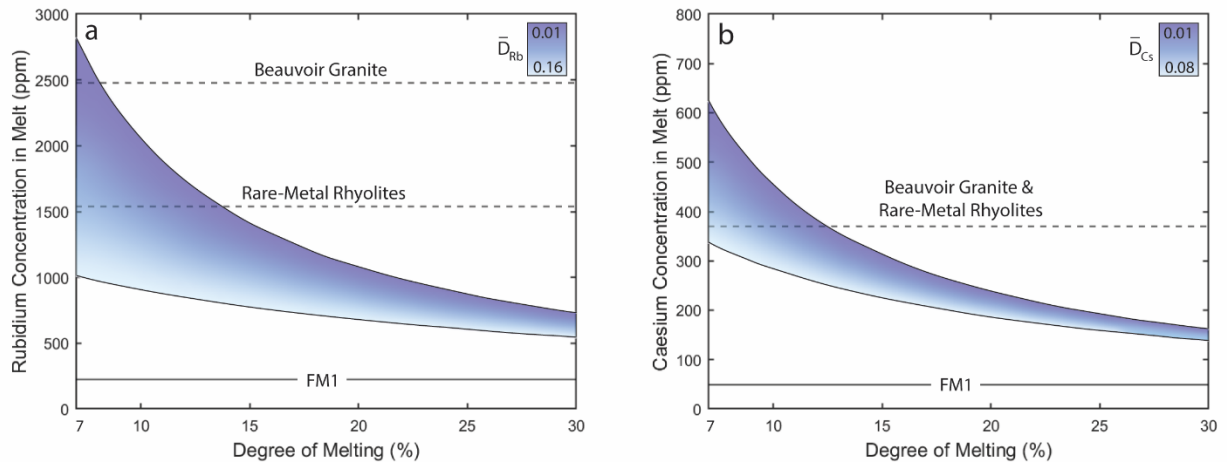
Supplementary Fig. 5 The normalised major element composition of the experimental glasses. The composition of the glasses was compared with melt compositions from previous experimental studies^{5,21,25}, rare-metal granites¹⁰, and rare-metal rhyolites¹⁸⁻²⁰ (Supplementary Data 2).



Supplementary Fig. 6 Sensitivity test of the trace element model to demonstrate the effect of variable $D_{Li}^{Mineral/Melt}$ on lithium enrichment during the partial melting of the FM1 micaschist. The degree of lithium enrichment during crustal anatexis is overestimated or underestimated using partition coefficients derived from granites and rhyolites, respectively.



Supplementary Fig. 7 Lithium enrichment during the partial melting of conventional metasedimentary rocks (20 ppm lithium) and the subsequent magmatic differentiation of low-degree (7%) partial melts. Event 1 highlights the partial melting of the metasedimentary source, whereas Events 2 and 3 reflect the magmatic differentiation of the extracted melts by fractional crystallisation or the re-melting of granitic cumulates. In the model, it is assumed that the partitioning behaviour of lithium is similar during crustal anatexis and fractional crystallisation. Therefore, 10% melting is considered to be the same as 90% crystallisation.



Supplementary Fig. 8 The enrichment of rubidium and caesium during anatexis. The enrichment of rubidium **(a)** and caesium **(b)** during the partial melting of the FM1 micaschist, assuming the complete breakdown of biotite and staurolite.

Supplementary References

1. Farrell, Ú. C. et al. The Sedimentary Geochemistry and Paleoenvironments Project. *Geobiology* **19**, 545–556 (2021).
2. Bowell, R. J., Lagos, L., de los Hoyos, C. R. & Declercq, J. Classification and characteristics of natural lithium resources. *Elements* **16**, 259–264 (2020).
3. Wu, Z. Advance review on occurrence state and leaching of lithium in sedimentary bauxite (aluminum) deposits, China. *Ore Geol. Rev.* **164**, 1-11 (2024).
4. Chappell, B.W. & White, A.J.R. I- and S-Type Granites in the Lachlan Fold Belt. *Earth Environ. Sci. Trans.* **83**, 1-26 (1974).
5. Patiño Douce, A. E. & Johnston, A. D. Phase equilibria and melt productivity in the pelitic system: implications for the origin of peraluminous granitoids and aluminous granulites. *Contributions Mineral. Petrol.* **107**, 202–218 (1991).
6. Goffé, B. Le facies a Carpholite-chloritoide dans la couverture briançonnaise des Alpes Lignes: un témoin de l'histoire tectono-metamorphique regional. *Mem. Soc. Geol. It.* **28**, 461–479 (1984).
7. Franceschelli, M., Puxeddu, M. & Memmi, I. Li, B-rich Rhaetian metabauxite, Tuscany, Italy: reworking of older bauxites and igneous rocks. *Chem. Geol.* **144**, 221–242 (1998).
8. Verlaquet, A. et al. Metamorphic veining and mass transfer in a chemically closed system: A case study in Alpine metabauxites (western Vanoise). *J. Metamorphic Geol.* **29**, 275–300 (2011).
9. Piantone, P. & Burnol, L. Géochimie des micaschistes du sondage d'Échassières. *Géol. Fr.* **2–3**, 295–309 (1987).
10. Linnen, R. L. & Cuney, M. Granite-related rare-element deposits and experimental constraints on Ta-Nb-W-Sn-Zr-Hf mineralization in *Rare-Element Geochemistry and*

Mineral Deposits (eds Linnen, R. L. & Samson, I. M.) 45-68 (Geological Association of Canada Short Course Notes 17, 2005).

11. Stilling, A., Černý, P. & Vanstone, P. J. The Tanco pegmatite at Bernic Lake, Manitoba. XVI. zonal and bulk compositions and their petrogenetic significance. *Can. Mineral.* **44**, 599–623 (2006).
12. Partington, G. A., Mcnaughton, N. J. & Williams, I. S. A review of the geology, mineralization, and geochronology of the Greenbushes pegmatite, Western Australia. *Econ. Geol.* **90**, 616–635 (1995).
13. Raimbault, L. Composition of complex lepidolite-type granitic pegmatites and of constituent columbite - tantalite, Chèdeville, Massif Central, France. *Can. Mineral.* **36**, 563–583 (1998).
14. Lamy Morissette, C., Cecchi, E. & Blais, J. F. Mineralogical variability of the Whabouchi pegmatite and its effect on the Li concentrations. *Can. Mineral.* **60**, 759–774 (2022).
15. Shaw, R. A. et al. The magmatic-hydrothermal transition in lithium pegmatites: petrographic and geochemical characteristics of pegmatites from the Kamativi area, Zimbabwe. *Can. Mineral.* **60**, 957–987 (2022).
16. London, D., Hervig, R. L. & Morgan, G. B. Melt-vapor solubilities and elemental partitioning in peraluminous granite-pegmatite systems: experimental results with Macusani glass at 200 MPa. *Contributions Mineral. Petrol.* **99**, 360–373 (1988).
17. Neukampf, J. & Ellis, B. Lithium loss from pegmatites controlled by country rock temperature. *Nat. Commun.* **16**, 1-2 (2025).
18. Pichavant et al. The Macusani glasses, SE Peru: evidence of chemical fractionation in peraluminous magmas in *Magmatic Processes: Physiochemical Principles* (ed Mysen, B. O.) 359-372 (The Geochemical Society, Special Publication No. 1, 1987).

19. Pichavant, M., Erdmann, S., Kontak, D. J., Michaud, J. A. -S. & Villaros, A. Trace element partitioning in strongly peraluminous rare-metal silicic magmas – implications for fractionation processes and for the origin of the Macusani Volcanics (SE Peru). *Geochim. Cosmochim. Acta* **365**, 229–252 (2024).
20. Raimbault, L. & Burnol, L. The Richemont rhyolite dyke, Massif Central, France: a subvolcanic equivalent of rare-metal granites. *Can. Mineral.* **36**, 265–282 (1998).
21. Pattison, D. R. M. & Spear, F. S. Kinetic control of staurolite–Al₂SiO₅ mineral assemblages: Implications for Barrovian and Buchan metamorphism. *J. Metamorphic Geol.* **36**, 667–690 (2018).
22. Dutrow, B. L., Holdaway, M. J. & Hinton, R. W. Lithium in staurolite and its petrologic significance. *Contributions Mineral. Petrol.* **94**, 496–506 (1986).
23. Chopin, C., Goffé, B., Ungaretti, L. & Obertie, R. Magnesio-staurolite and zinc-staurolite : mineral description with petrogenetic and crystal-chemical update. *Eur. J. Mineral.* **15**, 167–176 (2003).
24. García-Casco, A. et al. Synthesis of staurolite in melting experiments of a natural metapelite: Consequences for the phase relations in low-temperature pelitic migmatites. *J. Petrol.* **44**, 1727–1757 (2003).
25. Vielzeuf, D. & Montel, J. M. Partial melting of metagreywackes. Part I. Fluid-absent experiments and phase relationships. *Contributions Mineral. Petrol.* **117**, 375–393 (1994).
26. Montel, J.-M. & Vielzeuf, D. Partial melting of metagreywackes, Part II. Compositions of minerals and melts. *Contributions Mineral. Petrol.* **128**, 176–196 (1997).
27. Patiño Douce, A. E. & Harris, N. Experimental constraints on Himalayan anatexis. *J. Petrol.* **39**, 689–710 (1998).

28. Konzett, J., Hauzenberger, C., Ludwig, T. & Stalder, R. Anatectic granitic pegmatites from the eastern alps: A case of variable rare metal enrichment during high-grade regional metamorphism. II: Pegmatite staurolite as an indicator of anatectic pegmatite parent melt formation - a field and experimental study. *Can. Mineral.* **56**, 603–624 (2018).
29. Fockenberg, T. An experimental investigation on the P-T stability of Mg-staurolite in the system MgO-Al₂O₃-SiO₂-H₂O. *Contributions Mineral. Petrol.* **130**, 187-198 (1998).
30. Spear, F. S., Kohn, M. J. & Cheney, J. T. P-T paths from anatectic pelites. *Contributions Mineral. Petrol.* **134**, 17–32 (1999).
31. Knoll, T. et al. Lithium pegmatite of anatectic origin – A case study from the Austroalpine Unit Pegmatite Province (Eastern European Alps): geological data and geochemical modelling. *Ore Geol. Rev.* **154**, 1-32 (2023).
32. Hammouda, T. & Pichavant, M. Kinetics of melting of fluorophlogopite-quartz pairs at 1 atmosphere. *Eur. J. Mineral.* **11**, 637–653 (1999).
33. Rushmer, T. Volume change during partial melting reactions: implications for melt extraction, melt geochemistry and crustal rheology. *Tectonophysics* **342**, 389–405 (2001).
34. Michaud, J. A. S., Pichavant, M. & Villaros, A. Rare elements enrichment in crustal peraluminous magmas: insights from partial melting experiments. *Contributions Mineral. Petrol.* **176**, 1-33 (2021).
35. Sawyer, E. W. Disequilibrium melting and the rate of melt-residuum separation during migmatization of mafic rocks from the Grenville Front, Quebec. *J. Petrol.* **32**, 701-738 (1991).

36. Brown, M., Averkin, Y. A., McLellan, E. L. & Sawyer, E. W. Melt segregation in migmatites. *J. Geophys. Res.* **100**, 15655-15679 (1995).
37. Bea, F. Residence of REE, Y, Th and U in granites and crustal protoliths; implications for the chemistry of crustal melts. *J. Petrol.* **37**, 521-552 (1996).
38. Nabalek, P. Trace element distribution among rock-forming minerals in Black Hills migmatites, South Dakota: A case for solid-state equilibrium. *Am. Mineral.* **84**, 1256-1269 (1999).
39. Solar, G. S. & Brown, M. Petrogenesis of migmatites in Maine, USA: Possible source of peraluminous leucogranites in plutons? *J. Petrol.* **42**, 789-823 (2001).
40. Acosta-Vigil, A., London, D. & Morgan, G. B. Experiments on the kinetics of partial melting of a leucogranite at 200 MPa H₂O and 690-800°C: compositional variability of melts during the onset of H₂O-saturated crustal anatexis. *Contributions Mineral. Petrol.* **151**, 539-557 (2006).
41. Watson, E. B. & Müller, T. Non-equilibrium isotopic and elemental fractionation during diffusion-controlled crystal growth under static and dynamic conditions. *Chem. Geol.* **267**, 111-124 (2009).
42. Holtz, F. & Johannes, W. Genesis of peraluminous granites I. Experimental investigation of melt compositions at 3 and 3 kb and various H₂O activities. *J. Petrol.* **32**, 935-958 (1991).
43. Castro, A. et al. Origin of peraluminous granites and granodiorites, Iberian massif, Spain: an experimental test of granite petrogenesis. *Contributions Mineral. Petrol.* **135**, 255-276 (1999).
44. Gion, A. M., Piccoli, P. M., Fei, Y., Candela, P. A. & Ash, R. D. Experimental constraints on the formation of pegmatite-forming melts by anatexis of amphibolite: A case study from Evje-Iveland, Norway. *Lithos* **398–399**, 2-27 (2021).

45. Acosta-Vigil, A. et al. Mechanisms of crustal anatexis: A geochemical study of partially melted metapelitic enclaves and host dacite, SE Spain. *J. Petrol.* **51**, 785–821 (2010).
46. Holness, M. B., Cesare, B. & Sawyer, E. W. Melted rocks under the microscope: Microstructures and their interpretation. *Elements* **7**, 247-252 (2011).
47. Jambon, A. Tracer diffusion in granitic melts : Experimental results for Na, K, Rb, Cs, Ca, Sr, Ba, Ce, Eu, to 1300°C and a model of calculations. *J. Geophys. Res.* **87**, 10797-10810 (1982).
48. Zhang, Y., Ni, H. & Chen, Y. Diffusion data in silicate melts. *Rev. Mineral. Geochem.* **72**, 311-408 (2010).
49. Charlier, B. L. A. et al. Lithium concentration gradients in feldspar and quartz record the final minutes of magma ascent in an explosive supereruption. *Earth Planet. Sci. Lett.* **319-320**, 218-227 (2012).
50. Bea, F., Pereira, M. D. & Stroh, A. Mineral/leucosome trace-element partitioning in a peraluminous migmatites (a laser ablation –ICP-MS study). *Chem. Geol.* **117**, 291-312 (1994).
51. Macdonald, R., Smith, R. L. & Thomas, J. E. Chemistry of the subalkalic silicic obsidians in *U.S. Geological Survey Professional Paper 1523* 1-213 (United States Government Printing Office, Washington, 1992).
52. Raimbault, L., Cuney, M., Azencott, C., Duthou, J. L. & Joron, J. L. Geochemical evidence for a multistage magmatic genesis of Ta-Sn-Li mineralization in the granite at Beauvoir, French Massif Central. *Econ. Geol.* **90**, 548–576 (1995).
53. Linnen, R., McNeil, A. & Flemming, R. Some thoughts on metasomatism in pegmatites. *Can. Mineral.* **57**, 765-766 (2019).

54. Schmidt, M. W., Dardon, A., Chazot, G. & Vannucci, R. The dependence of Nb and Ta rutile-melt partitioning on melt composition and Nb/Ta fractionation during subduction processes. *Earth Planet. Sci. Lett.* **226**, 415-432 (2004).
55. Paparoni, G., Webster, J. D. & Walker, D. Experimental techniques for determining tin solubility in silicate melts using silica capsules in 1 atm furnaces and rhenium capsules in the piston-cylinder. *Am. Mineral.* **95**, 776-783 (2010).
56. Bindeman, I. N., Davis, A. M. & Drake, M. Ion microprobe study of plagioclase-basalt partition experiments at natural concentration levels of trace elements. *Geochim. Cosmochim. Acta* **62**, 1175–1193 (1998).
57. Bindeman, I. N. & Davis, A. M. Trace element partitioning between plagioclase and melt: Investigation of dopant influence on partition behaviour. *Geochim. Cosmochim. Acta* **64**, 2863–2878 (2000).
58. Aigner-Torres, M., Blundy, J., Ulmer, P. & Pettke, T. Laser Ablation ICPMS study of trace element partitioning between plagioclase and basaltic melts: An experimental approach: *Contributions Mineral. Petrol.* **153**, 647–667 (2007).
59. Tepley, F. J., Lundstrom, C. C., McDonough, W. F. & Thompson, A. Trace element partitioning between high-An plagioclase and basaltic to basaltic andesite melt at 1 atmosphere pressure. *Lithos* **118**, 82–94 (2010).
60. Sun, C., Graff, M., & Liang, Y. Trace element partitioning between plagioclase and silicate melt: The importance of temperature and plagioclase composition, with implications for terrestrial and lunar magmatism: *Geochim. Cosmochim. Acta* **206**, 273–295 (2017).
61. Haupt, C. P. et al. Trace element partitioning in the lunar magma ocean: an experimental study: *Contributions Mineral. Petrol.* **179**, 1-23 (2024).